

**This item is the archived peer-reviewed author-version of:**

Does the wet addition of crumb rubber and emission reduction agents impair the rheological performance of bitumen?

**Reference:**

Bressan Borinelli Jaffer, Blom Johan, Vuye Cedric, Hernando David.- Does the wet addition of crumb rubber and emission reduction agents impair the rheological performance of bitumen?  
Construction and building materials - ISSN 1879-0526 - 417(2024), 135351  
Full text (Publisher's DOI): <https://doi.org/10.1016/J.CONBUILDMAT.2024.135351>  
To cite this reference: <https://hdl.handle.net/10067/2031880151162165141>

# 1 Does the wet addition of crumb rubber and emission reduction agents 2 impair the rheological performance of bitumen?

3 **Abstract:** Crumb rubber modified bitumen (CRMB) is a promising solution for  
4 recycling waste tyres and improving asphalt performance. Nonetheless, higher  
5 temperatures are usually required during mixing, which increases the emission of  
6 volatile organic compounds (VOCs) that can potentially cause harmful health  
7 effects on workers due to their toxic and carcinogenic properties. Emission  
8 reduction agents (ERAs) have been developed to address this issue. However,  
9 limited scientific evidence is available regarding their impact on the rheological  
10 performance of CRMB, which makes the selection of the most suitable ERA  
11 challenging. This study investigated the effects of three ERAs on the physical and  
12 rheological properties of CRMB: steam-activated carbon/charcoal (AC), fly ash-  
13 based geopolymer (GFA), and Portland cement paste (PCP). In addition to  
14 penetration and softening point tests, a dynamic shear rheometer (DSR) was used  
15 to evaluate the rheological properties of the samples in the frequency and  
16 temperature domains and to perform the multiple stress creep recovery (MSCR)  
17 and linear amplitude sweep (LAS) tests. The results revealed that the three ERAs  
18 increased the stiffness of CRMB: penetration reduced and softening point,  
19 penetration index, and viscosity increased. This stiffening effect caused a drop in  
20 the fatigue resistance measured in the LAS test. Out of the three ERAs evaluated,  
21 AC clearly induced the greatest changes in binder properties. However, MSCR  
22 results, crossover frequency, R-value, Glover-Rowe parameter, and  $\Delta T_c$  were less  
23 sensitive to the addition of ERAs. It was concluded that the addition of GFA and  
24 PCP did not impair the physical and rheological properties of CRMB, yielding  
25 results comparable to those of a PMB. However, AC may introduce issues during  
26 mixing and service life due to the increase in viscosity and the reduction in fatigue  
27 resistance.

28 **Keywords:** volatile organic compounds; crumb rubber modified bitumen;  
29 emission reduction agents; physical and rheological parameters

# Does the wet addition of crumb rubber and emission reduction agents impair the rheological performance of bitumen?

## 1. Introduction

Global tyre production reached 19 million tons in 2019 [1]. According to the European Tyre Rubber Manufacturers Association, 5.1 million tonnes of tyres were produced in the European Union in 2020 [2]. In addition, millions of used tyres reach the end of their service life every year and fall into the category of end-of-life tyres (ELTs) [3]. The rubber employed in the fabrication of tyres is very resilient, which leads to a great potential to be reused. Alternative final destinations for ELTs are explored since landfill disposal has been banned in most countries. Reusing and recycling are preferable options for this high-quality material as it can be used to reduce the consumption of raw materials. Due to governmental support in Europe for recycling and increasing concerns about waste growth, new end markets are being developed to find a better destination for ELTs [4]. One solution is the development of rubberised bitumen for road construction using tyre-derived crumb rubber (CR) from ELTs to address pavement performance issues and tackle the disposal problem of ELTs. CR blended into bitumen is considered to improve asphalt pavement performance in terms of high-temperature stability, fatigue life and cracking resistance, and a solution for waste tyre recycling technology [5-7].

Nonetheless, incorporating CR into bituminous mixtures raises certain issues, such as limited pumpability, mixability, and workability, as well as the need for additional energy to heat the materials during the mixing and compaction processes [8]. The interaction between CR and bitumen is a physical interaction, characterized by the absorption of the aromatic fraction (maltenes) of the binder by the CR through diffusion. This occurs as the maltenes of the bitumen and CR exhibit similar solubility parameters, which leads to

25 enhanced compatibility between them [9]. The absorption of maltenes combined with a  
26 decrease in the oily fraction of the binder causes the CR particles to swell, which increases  
27 the viscosity of crumb rubber modified bitumen (CRMB) [10].

28 To overcome the increase in viscosity, asphalt mixtures using CRMB require a higher  
29 temperature than those with a traditional binder. This leads to an increase in the emission  
30 of fumes, odour, and volatile organic compounds (VOCs) like toluene, ethylbenzene,  
31 xylenes, and sulphur compounds [11-15], which poses a risk to pavement construction  
32 workers and also affects the growth and development of animals and plants [16-19].  
33 Higher temperatures stimulate molecular movement and release lighter compounds [20,  
34 21]. To reduce fume emissions, warm mix additives and emission reduction agents  
35 (ERAs) have gained attention in recent years. Warm mix technology (either with  
36 additives or using foamed bitumen) aims to reduce the viscosity of the binder and allows  
37 for a lower mixing temperature compared to hot mix asphalt. Turbay et al. [22] conducted  
38 a rheological analysis to evaluate the behaviour of CRMB when modified with warm mix  
39 additives, specifically Evotherm M1 and Iterlow T, at a dosage of 0.3% by weight of  
40 bitumen. They concluded that the use of these additives tend to slightly decrease the  
41 viscosity, stiffness and performance at high temperature of CRMB. Worse high  
42 temperature performance was also reported by Yu et al. [23] when creating foamed  
43 CRMB with different water contents. Although warm mixtures have been found to reduce  
44 the emission of VOCs, polycyclic aromatic hydrocarbons, and total suspended particles,  
45 this may come at the expense of the final performance [24]. For that reason, the addition  
46 of ERAs could be a solution to effectively reduce emissions with limited effect on  
47 performance. Despite the importance of effectively reducing VOCs, there have been  
48 limited studies about the impact of ERAs on the rheology of the binder. Cui et al. [25]  
49 used 4 wt% styrene butadiene styrene (SBS) and 4 wt% active carbon filler as ERA, and

50 concluded that the combination of both materials significantly lowered the VOC emission  
 51 and improved the deformation resistance at higher temperatures. Wu et al. [26] used  
 52 mesoporous hollow silica as ERA and observed an increase in complex modulus and a  
 53 decrease in phase angle and rutting factors while reducing the VOC emission. The  
 54 scarcity of such studies has prompted us to explore this area thoroughly and provide  
 55 valuable scientific evidence to aid in selecting the most suitable ERA for effectively  
 56 reducing VOC emissions while maintaining optimal binder performance.

## 57 **2. Objectives and scope**

58 The objective of this study is to investigate the impact of ERAs on the physical and  
 59 rheological properties of CRMB. In addition, a comparative analysis with commercially  
 60 available unmodified (base) and polymer-modified bitumen (PMB) was conducted to  
 61 offer insights into the advantages and potential drawbacks of utilizing CR and different  
 62 ERAs for improving binder performance while reducing VOC emissions.

63 Steam-activated carbon/charcoal (AC), fly ash-based geopolymer (GFA), and Portland  
 64 cement paste (PCP) were selected as ERAs based on their potential to reduce VOC  
 65 emissions from CRMB evaluated in a prior study [15]. Table 1 shows the summary of the  
 66 results obtained in the prior study for total VOC emission (TVOC) rate considering all  
 67 measured VOCs, most significant VOCs released when CR was added to the binder, and  
 68 VOCs classified as health hazards, acute toxic or environmental hazards according to the  
 69 Globally Harmonized System of Classification and Labelling of Chemicals (GHS) [27].

70 Table 1. VOC emission rate for CR modified bitumen blends (in  $\mu\text{mol}/\text{m}^2$ ) [15]

	<b>TVOC*</b>	<b>Hazardous VOCs**</b>	<b>CR VOCs***</b>
Base	60.0	42.0	25.4
PMB	114.9	92.6	63.8
CRMB	108.2	78.8	65.7
CRMB+AC	55.4	34.2	26.9

	TVOC*	Hazardous VOCs**	CR VOCs***
CRMB+GFA	56.5	34.8	21.7
CRMB+PCP	45.3	30.0	21.0

71 \* TVOC: total VOC emission rate considering all VOCs measured

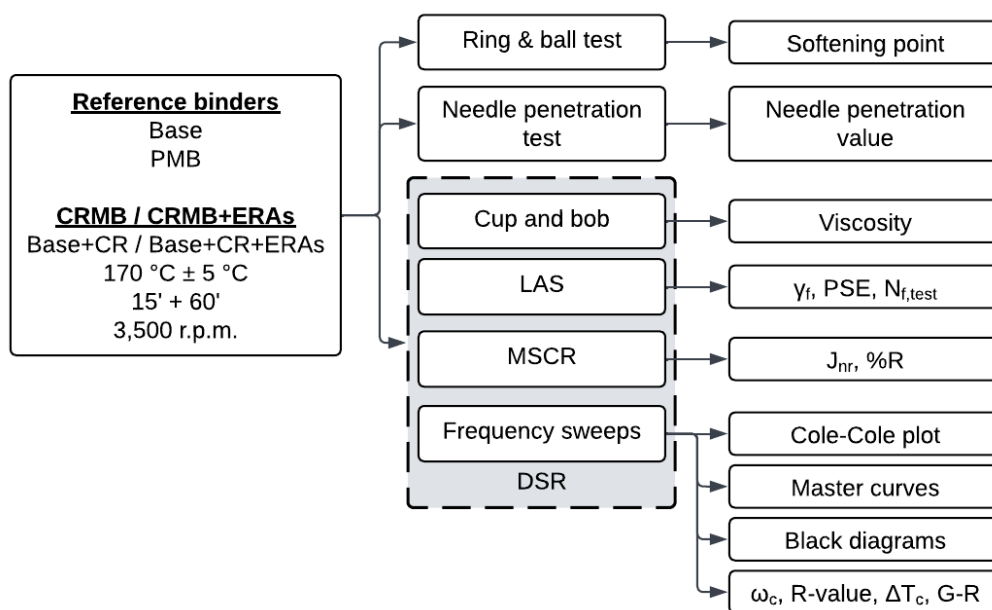
72 \*\* Hazardous VOCs: classified as health hazards, acute toxic or environmental hazards according to the  
73 GHS

74 \*\*\*CR VOC: most significant VOCs released when CR was added to a base bitumen

75 Note: all samples were heated up to 180 °C over 320s

### 76 3. Materials and Methods

77 This study comprised a combination of empirical and rheological tests to evaluate the  
78 impact of ERAs on the performance of CRMB. The experimental methods are illustrated  
79 in Figure 1 and described in detail in the following subsections. The physical  
80 characteristics were determined by means of standard penetration and softening point  
81 tests. A dynamic shear rheometer (DSR) was used to evaluate the rheological properties  
82 of the samples in the frequency and temperature domains and to perform the multiple  
83 stress creep recovery (MSCR) and linear amplitude sweep (LAS) tests. Comparisons  
84 were also made with unmodified virgin bitumen and a commercially available polymer-  
85 modified bitumen (PMB).



86

87

Figure 1. Flowchart of the experimental method

88 **3.1. VOC emission reduction agents**

89 Steam-activated carbon/charcoal was supplied by Alfa Aesar. Ordinary Portland cement  
 90 (OPC) was provided by Sibelco and was activated using distilled water to create a  
 91 Portland cement paste (PCP). Fly ash (FA) class F, supplied by Value Ash Technologies,  
 92 was used as precursor material to synthesise the geopolymer-based additive. The alkaline  
 93 activator was composed of sodium hydroxide (98% pure, pellets) and a sodium silicate  
 94 solution (initial composition of 25.9 wt.% of sodium oxide, 7.9 wt.% of silicon oxide, and  
 95 66.2% water). Table 2 shows the formulation of the FA-based geopolymer (GFA) paste  
 96 and PCP paste. PCP and GFA were then sealed and placed in an oven at 60 °C for 3 days.  
 97 Before being used, AC, GFA, and PCP were milled and the fraction passing the 0.125  
 98 mm sieve was selected.

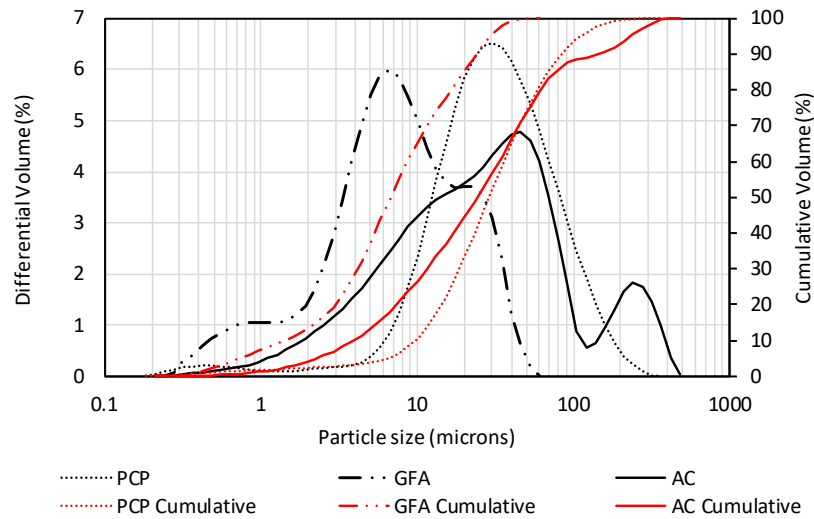
99

Table 2. Paste formulation

	<b>FA (g)</b>	<b>OPC (g)</b>	<b>NaOH (g)</b>	<b>Na<sub>2</sub>SiO<sub>3</sub> (g)</b>	<b>Water (g)</b>
GFA	45.00	-	1.38	9.43	11.45
PCP	-	45.00	-	-	18.00

100

101 A Mastersizer Hydro 2000G Particle Size Analyser (Malvern, UK) was used to measure  
 102 the differential and cumulative volumes for each ERA and these results are shown in  
 103 Figure 2. To disperse the agglomerates, the powders were subjected to ultrasonic  
 104 agitation. The results showed that GFA had the smallest mean particle size (6.71 µm),  
 105 followed by AC (24.87 µm) and PCP (28.71 µm).



106

107 Figure 2. Differential (in black) and cumulative (in red) volumes of the emission  
108 reduction agents.

### 109 3.2 Bitumen

110 A unmodified bitumen (base) with a pen grade of 50/70 was used as the base binder for  
111 crumb rubber modification, and a polymer modified bitumen (PMB) with a grade of  
112 10/40-65 was used for comparison purposes. Both binders are readily available in the  
113 Belgian market, with the PMB being formulated through the crosslinking of bitumen and  
114 a thermoplastic elastomer. The penetration values, softening points, and penetration  
115 indices of both binders are reported in Table 3.

116 Table 3. Mechanical properties of the reference binders

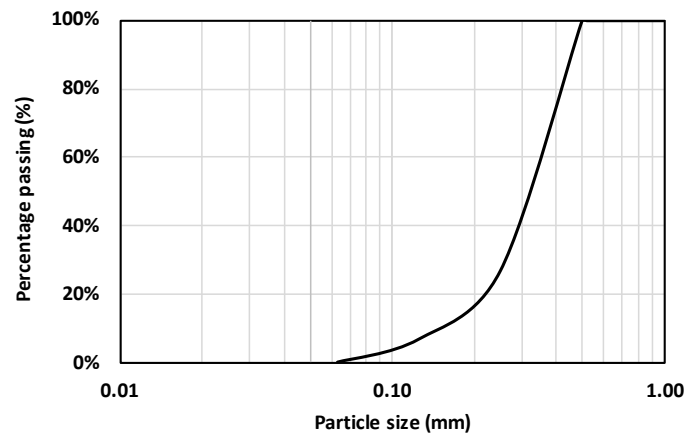
Property	Test Standard	Results		Unit
		Base	PMB	
Penetration (at 25 °C)	EN 1426	53.0	21.0	0.1 mm
Softening point	EN 1427	51.8	69.0	°C
Penetration index	-	- 0.6	0.7	-

### 117 3.3 Crumb rubber

118 The base bitumen was modified with a crumb rubber source produced by ambient  
119 grinding. This process leads to irregularly shaped particles with relatively high surface



120 area, which improves the interaction between CR and binder [5]. Figure 3 displays that  
121 the CR fraction used for bitumen modification passed the 0.5 mm sieve.



122

123 Figure 3. Gradation curve of the fraction of the CR used to modify the base binder

124 A Q50000IR Thermogravimetric Analyzer (TA Instruments) was used to determine the  
125 following composition of CR by weight: 9.14% oils and volatiles, 53.73% natural and  
126 synthetic rubber, 28.51% carbon black, and 8.62% inert filler.

### 127 **3.4 Blending process**

128 The crumb rubber modified bitumen (CRMB) was prepared by blending the base  
129 bitumen (500 g) at  $170\text{ }^{\circ}\text{C} \pm 5\text{ }^{\circ}\text{C}$  with the CR particles. Previous studies consistently  
130 reported that the typical rubber content in CRMB ranges between 10% to 20% by weight  
131 of the bitumen [28-30]. The decision to include 15% of CR by mass of bitumen was  
132 informed by prior findings [31], which demonstrated that this proportion resulted in  
133 reduced temperature susceptibility and enhanced binder elasticity. To ensure proper  
134 digestion of the CR into the bituminous matrix, a high shear mixer with a speed of  
135 3,500 r.p.m. was employed for 75 min (15 min to reach temperature equilibrium followed  
136 by 60 min at  $170\text{ }^{\circ}\text{C} \pm 5\text{ }^{\circ}\text{C}$ ). A heating mantle was utilised to keep the temperature at  
137  $175\text{ }^{\circ}\text{C}$ . For blends with ERAs, the ERA was incorporated into the bitumen prior to the

138 addition of CR, with a mass ratio of 5.75% relative to the bitumen. The ERA ratio of  
 139 5.75% by weight of bitumen was explored in previous studies [15, 32, 33]. The samples  
 140 were labelled as presented in Table 4.

141 Table 4. Summary of the bituminous blends and their composition (% by mass of  
 142 bitumen)

Name	CR content	ERA content	ERA type
CRMB	15.0	-	-
CRMB+AC	15.0	5.75	Steam-activated carbon/charcoal
CRMB+GFA	15.0	5.75	Ground granulated blast furnace slag-based geopolymer
CRMB+PCP	15.0	5.75	Portland cement paste

### 143 3.5. Experimental methods

#### 144 3.5.1 Empirical binder tests

145 Softening point and needle penetration values were determined according to  
 146 EN 1427:2015 and EN 1426:2015, respectively. In order to obtain a quantitative  
 147 measurement of temperature susceptibility, the penetration index (PI) was calculated  
 148 based on the softening point (SP) and penetration values at 25 °C (PEN) following Eq.  
 149 (1) [34].

$$PI = \frac{1952 - 500 \log(PEN) - 20 SP}{50 \log(PEN) - SP - 120} \quad (1)$$

#### 150 3.5.2 Rheological tests

##### 151 Viscosity – High temperature

152 The viscosity of bitumen at high temperatures is considered a vital property as it  
 153 represents the binder's mixability, pumpability, and workability. A bob and cup feature  
 154 was used in the DSR to measure the viscosity in accordance with EN 13302 in a

155 temperature range from 135 to 177.5 °C. Unmodified binders generally behave like a  
156 Newtonian fluid, where their viscosities are independent of the shear rates. On the other  
157 hand, modified binders normally show a non-Newtonian behaviour that is dependent on  
158 shear rate and temperature, with viscosities decreasing as the shear rate increases [35].  
159 For that reason, a prolonged period was adopted before taking the readings in a range of  
160 shear rates from 1 to 100 s<sup>-1</sup> at 5 s<sup>-1</sup> intervals. For comparison purposes, the specific shear  
161 rate highlighted in this study corresponds to 100 s<sup>-1</sup> for all temperatures, representing the  
162 region where the blends demonstrate a Newtonian behaviour.

163 The viscous behaviour of the binder can be attributed to a thermally activated process,  
164 where molecules must overcome energy barriers to move within the material. The  
165 intermolecular forces during the flow of asphalt create resistance, and this resistance is  
166 governed by the activation energy, which represents the minimum energy required to  
167 overcome it. The determination of this energy can help understand if the incorporation of  
168 crumb rubber as a modifier changes the thermally activated resistance of the base binder  
169 [36]. The Arrhenius model, Equation (2), was used to determine the activation energy,  
170 where  $\eta$  is the viscosity of the bituminous binder, T is the temperature in degree Kelvin,  
171 A is a model constant, R is the universal gas constant (8.314 J·mol<sup>-1</sup>·K<sup>-1</sup>), and E<sub>f</sub> is the  
172 activation energy. A more concise representation of Equation (2) is shown in Equation  
173 (3), where the slope of ln ( $\eta$ ) versus 1/T is equal to E<sub>f</sub>/R, given the linear trend observed.

$$\eta = Ae^{\frac{E_f}{RT}} \quad (2)$$

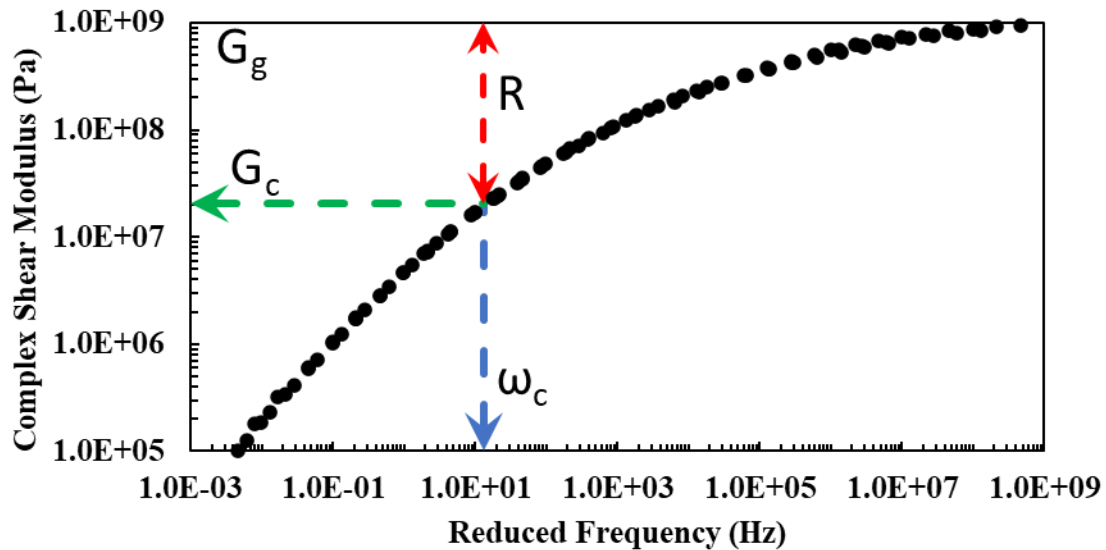
$$\ln \eta = \frac{E_f}{RT} + \ln A \quad (3)$$

174 Frequency sweeps

175 To evaluate the effect of the ERAs on the rheological properties of CRMB, frequency  
 176 sweeps were conducted on unaged samples using a dynamic shear rheometer (DSR) from  
 177 Anton Paar. For the high frequency-low temperature range (-30 °C to +10 °C), a 4 mm  
 178 parallel plate geometry with a 1.75 mm gap was utilised. For the higher temperature  
 179 ranges of 0 to +40 °C and +30 to +70 °C, parallel plates were utilised with gaps of 2 and  
 180 1 mm, and diameters of 8 and 25 mm, respectively. Frequency sweeps ranging from 0.1  
 181 to 10 Hz were conducted under strain control. Optimal strain levels of 0.05% and 1%  
 182 were used for performing strain-controlled frequency sweeps within the linear  
 183 viscoelastic region for the 8 mm and 25 mm plates, respectively. The storage (G') and  
 184 loss moduli (G'') measured by the DSR were utilised to calculate the complex shear  
 185 modulus (G\*) and phase angle (δ).

186 Master curves were built by processing the raw data with the rheological software  
 187 RHEA™ (by Abatech Engineering Consultants [37]). The Christensen-Anderson (CA)  
 188 mathematical model was used to build the master curves at a reference temperature of  
 189 15 °C [38, 39]. The CA model, Equation (4), defines the complex shear modulus (G\*) as  
 190 a function of frequency based on the glassy modulus (G<sub>g</sub>), the rheological shape  
 191 parameter (R), and the crossover frequency (ω<sub>c</sub>), which is the frequency at which G' and  
 192 G'' are equal. The difference between the log of G<sub>g</sub> and the crossover modulus (G<sub>c</sub>), where  
 193 G'=G''=G<sub>c</sub>, is expressed by the shape parameter R. While the R parameter expresses the  
 194 variation in relaxation properties, ω<sub>c</sub> indicates the transition point between an elastic and  
 195 a more viscous behaviour [40]. A graphical representation of the parameters defined in  
 196 the CA model is shown in Figure 4.

$$G^*(\omega) = G_g * \left[ 1 + \frac{\omega_c^{(\log 2/R)}}{\omega} \right]^{-R/\log 2} \quad (4)$$



197

198 Figure 4. Graphical representation of the glassy modulus ( $G_g$ ) the rheological shape  
 199 parameter ( $R$ ), and the crossover frequency ( $\omega_c$ ).

200 The Black diagram is a representation of the raw rheological data and is commonly used  
 201 to evaluate the impact of polymer modification on the rheological characteristics of a  
 202 modified bitumen. This diagram is generated by collecting the phase angle and complex  
 203 shear modulus under various temperature and frequency conditions. When examining the  
 204 diagram, a smooth curve indicates a binder that exhibits the expected response of time-  
 205 temperature equivalence, which is typically observed in unmodified binders. Conversely,  
 206 discontinuities within the diagram suggest the presence of bitumen with high wax content,  
 207 highly polymer modified bitumen, or a binder with a highly asphaltene structured  
 208 composition [41].

209 The Glover-Rowe (G-R) parameter is associated with fatigue cracking [42]. It is  
 210 calculated according to Equation (5) using the  $G^*$  and  $\delta$  measured at a test temperature  
 211 of 15 °C and a frequency of 0.005 rad/s [43]. In this study, the G-R parameter was  
 212 estimated from the RHEA™ software based on the full CA master curves. Two damage  
 213 thresholds have been proposed for the G-R parameter:  $G-R = 180$  kPa suggests onset

214 cracking (warning) and  $G-R = 600$  kPa indicates significant cracking (critical) [44].  
215 Higher values of  $G-R$  indicate more brittle asphalt binders that are more susceptible to  
216 fatigue cracking, as it has been demonstrated in other studies [45-47]. The  $G-R$  thresholds  
217 should be understood as an indication of possible crack formation, rather than being  
218 regarded as an absolute classification criterion, considering the specific circumstances for  
219 which they were identified.

$$G-R = \frac{G^* * (\cos \delta)^2}{\sin \delta} \quad (5)$$

220  $\Delta T_c$  – Low temperature

221 As the frequency sweep measurements covered the low-temperature range (up to  $-30$  °C),  
222 an extra analysis was conducted to evaluate blend behaviour at lower temperatures.  
223 Instead of relying on the conventional bending beam rheometer (BBR) method, the  
224 relaxation parameter  $m$ -value and creep stiffness  $S(t)$  were derived from low-temperature  
225 DSR data [48, 49]. These parameters play a crucial role in determining  $\Delta T_c$ , a proposed  
226 indicator of both ageing-induced cracking and the evolution of ageing processes [47]. In  
227 a BBR test, the two lower continuous grading temperatures,  $T_{c,s}$ , and  $T_{c,m}$ , are determined  
228 by a stiffness  $G$  of 300 MPa and a slope ( $m$ ) of 0.3 at 60 s, respectively. However, the  
229 following conversions proposed by Christensen et al. [48] need to be applied when  
230 estimating  $\Delta T_c$  from DSR tests:  $G = 143$  MPa and  $m = 0.275$  at 60 s. As per the  
231 aforementioned studies, this conversion yields a satisfactory correlation between BBR  
232 and DSR measurements. The determination of the continuous grading temperatures,  $T_{c,G}$ ,  
233 and  $T_{c,m}$ , was carried out by applying Equations (6) and (7), respectively, in accordance  
234 with the procedures specified in ASTM D7643-16. As outlined in the standard, the  
235 temperature difference between these values, denoted as  $\Delta T_c$  — Equation (8). Two

236 relaxation moduli ( $G_1$  and  $G_2$ ) and two relaxation slopes ( $m_1$  and  $m_2$ ) at two temperatures  
 237 ( $T_1$  and  $T_2$ ) must be determined, where  $G_1 \leq 143 \text{ MPa} \leq G_2$  and  $m_1 \leq 0.275 \leq m_2$ . Binders  
 238 with lower (i.e., more negative)  $\Delta T_c$  values are more susceptible to thermal cracking, as  
 239 they exhibit lower stress relaxation properties. Two limits have been proposed for  $\Delta T_c$  as  
 240 performance indicators:  $-2.5 \text{ }^\circ\text{C}$  and  $-5 \text{ }^\circ\text{C}$  as warning and critical limits, respectively  
 241 [47]. In accordance with ASTM D7643-16, the samples were short- and long-term aged  
 242 using the rolling thin film oven (RTFO, EN 12607-1) test at a temperature of  $163 \text{ }^\circ\text{C}$  for  
 243 75 min, followed by the pressure ageing vessel (PAV, EN14769) test, at a temperature of  
 244  $100 \text{ }^\circ\text{C}$  and air pressure of  $2.1 \text{ MPa}$  for 20 h.

$$T_{c,G} = T_1 + \frac{(T_1 - T_2) * (\log 143 + \log G_1)}{\log G_1 - \log G_2} - 10 \quad (6)$$

$$T_{c,m} = T_1 + \frac{(T_1 - T_2) * (0.275 + m_1)}{m_1 - m_2} - 10 \quad (7)$$

$$\Delta T_c = T_{c,G} - T_{c,m} \quad (8)$$

245 Linear amplitude sweep (LAS) – Intermediate temperature

246 In order to evaluate the fatigue resistance of the blends, the LAS test was performed. It  
 247 has been proposed as an alternative to the fatigue parameter  $G^* \cdot \sin \delta$  introduced by  
 248 SHRP, as this was later found to have a poor correlation with the fatigue performance of  
 249 asphalt mixtures [50]. Conversely, the bitumen fatigue life estimated from the LAS test  
 250 has shown a reliable correlation with the fatigue resistance of asphalt mixtures [51, 52].  
 251 As described in AASHTO TP 101, the LAS test is performed on a DSR equipped with an  
 252 8 mm parallel plate geometry at a constant temperature ( $15 \text{ }^\circ\text{C}$  for this study) on samples

253 after RTFO+PAV. The first stage of the LAS test is a frequency sweep from 0.2 to 30 Hz  
254 to define the undamaged properties and the damage evolution parameter at a strain level  
255 of 0.1 % (to ensure the binder strain is within the linear viscoelastic region). The second  
256 stage is the linear amplitude strain sweep from 1 % to 30 % over 3000 cycles at 10 Hz.  
257 The failure criterion used in the LAS test was the peak in stored pseudo strain energy  
258 (PSE), which indicates a loss in the material's capacity to store additional PSE as strain  
259 increases [53]. The number of cycles corresponding to the peak in stored PSE ( $N_{f,test}$ ) was  
260 selected as the binder performance parameter in the LAS test [54].

261 Rutting Resistance Indicator (MSCR test) – High temperature

262 The MSCR test was introduced as a promising method to examine the elasticity and stress  
263 dependence of modified binders. The MSCR test was performed in accordance with  
264 EN 16659 at 50 °C. The temperature selection for this test was based on its  
265 correspondence to the rutting test temperature specific to the Flemish region in Belgium.  
266 The entire series of binders were short-term aged using the RTFO test. A 25 mm parallel  
267 plate geometry with a 1 mm gap setting was used and the samples were loaded at a  
268 constant stress for 1 s followed by 9 s of recovery. The stress levels of 0.1 kPa and 3.2 kPa  
269 were applied on each sample over ten cycles, and two main parameters were calculated:  
270 the non-recoverable creep compliance ( $J_{nr}$ ) and recovery percent (R%).  $J_{nr}$  is the ratio  
271 between the residual strain and the stress applied and has been proposed as an alternative  
272 for the traditional rutting parameter ( $G^*/\sin \delta$ ). R% represents the amount of strain  
273 recovered by the binder after repeated loading and unloading.

#### 274 **4. Results and discussion**

275 Table 5 presents a comprehensive summary of all binder test results. This table  
276 will be instrumental in facilitating the subsequent discussion of the results.



Table 5. Physical and rheological properties of all blends

Tests	Parameters	Condition	Units	Base	PMB	CRMB	CRMB+AC	CRMB+GFA	CRMB+PCP
<b>Empirical</b>	Penetration at 25 °C	Unaged	0.1 mm	53.0	21.0	34.0	27.0	30.0	30.0
	Softening point	Unaged	°C	51.8 ± 0.1	69.0 ± 0.1	64.6 ± 0.1	68.8 ± 0.2	65.2 ± 0.2	65.4 ± 0.2
	Penetration index	Unaged	-	-0.6	0.7	1.0	1.2	0.8	0.8
<b>Viscosity</b>	Dynamic viscosity at 135.0°C	Unaged	Pa·s	0.68 ± 0.01	3.21 ± 0.01	2.62 ± 0.02	4.09 ± 0.01	2.84 ± 0.03	2.84 ± 0.01
	Dynamic viscosity at 177.5°C	Unaged	Pa·s	0.11 ± 0.01	0.37 ± 0.01	0.44 ± 0.01	0.65 ± 0.01	0.46 ± 0.01	0.46 ± 0.01
	Activation energy (E <sub>f</sub> )	Unaged	kJ/mol	67.83	74.70	70.05	71.71	71.08	71.03
<b>Frequency sweeps</b>	Crossover frequency ( $\omega_c$ )	Unaged	Hz	12.87 ± 0.38	0.28 ± 0.01	0.21 ± 0.01	0.13 ± 0.01	0.22 ± 0.01	0.2 ± 0.02
	R-Value	Unaged	-	1.75 ± 0.01	2.23 ± 0.01	2.68 ± 0.02	2.73 ± 0.01	2.67 ± 0.01	2.70 ± 0.01
	G-R	Unaged	kPa	2.60 ± 0.3	53.35 ± 2.53	40.53 ± 0.41	67.68 ± 3.33	45.84 ± 1.16	48.19 ± 3.62
	T <sub>c,G</sub>	RTFO+PAV	°C	-16.59 ± 0.67	-12.04 ± 0.35	-23.27 ± 0.74	-22.23 ± 0.25	-21.03 ± 0.38	-22.53 ± 0.08
	T <sub>c,m</sub>	RTFO+PAV	°C	-13.70 ± 0.24	-7.66 ± 0.10	-14.47 ± 0.43	-13.85 ± 0.47	-13.60 ± 0.10	-13.75 ± 0.17
	$\Delta T_c$	RTFO+PAV	°C	-2.89 ± 0.42	-4.38 ± 0.25	-8.80 ± 0.31	-8.38 ± 0.22	-7.43 ± 0.38	-8.77 ± 0.09
	$\gamma_f$	RTFO+PAV	%	14.70	14.40	19.40	13.50	17.10	15.50
<b>LAS</b>	Maximum stored PSE	RTFO+PAV	-	3.37	6.62	1.76	1.73	1.69	1.66
	N <sub>f,test</sub>	RTFO+PAV	Cycles	1400	1370	1890	1280	1650	1490
<b>MSCR</b>	J <sub>nr 0.1</sub>	RTFO	1/kPa	2.30	0.56	0.59	0.53	0.62	0.52
	J <sub>nr 3.2</sub>	RTFO	1/kPa	2.34	0.55	0.62	0.54	0.64	0.51
	R <sub>0.1</sub>	RTFO	%	53.71	76.26	83.56	83.81	83.09	83.29
	R <sub>3.2</sub>	RTFO	%	52.62	76.88	82.84	83.44	82.48	83.32

#### 279 ***4.1. Empirical binder tests***

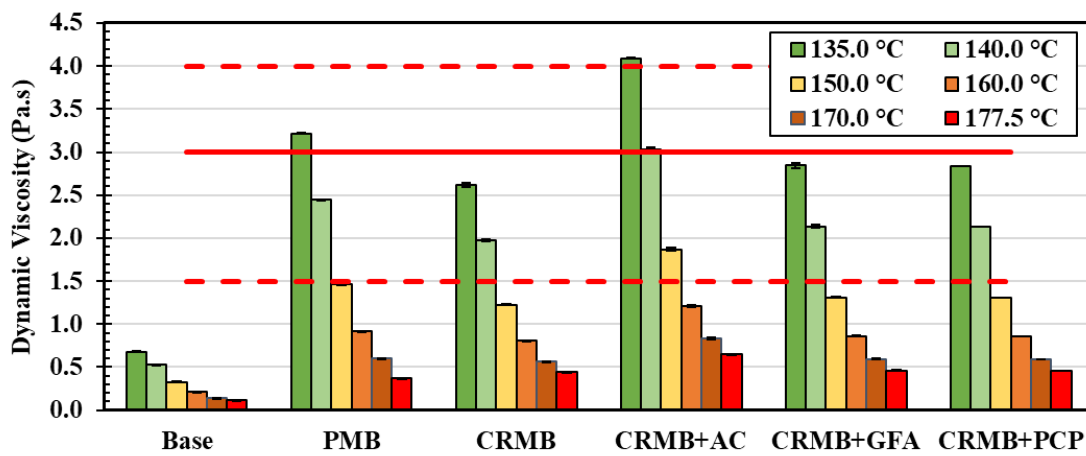
280 The results of the penetration and softening point tests are shown in Table 5. The  
281 incorporation of CR reduced the penetration value (the binder became stiffer) and  
282 increased the softening point to a level closer to that of PMB. The effect of polymer  
283 modification can be observed by the positive PI. The addition of ERAs led to a reduction  
284 in penetration levels and an increase in the softening point compared to CRMB. This  
285 trend aligns with the findings from Tang et al. [55], who observed a similar effect when  
286 adding geopolymer additives (6% by weight of bitumen) to an unmodified binder. The  
287 incorporation of AC to the blend resulted in a higher PI due to a lower penetration value  
288 and a higher SP. GFA and PCP showed similar results between each other and closer to  
289 those of CRMB.

#### 290 ***4.2. Rheological tests***

##### 291 *Viscosity*

292 Figure 5 shows the dynamic viscosity of the samples measured at different temperatures.  
293 The base binder behaved like a Newtonian fluid, whose viscosity is independent of the  
294 shear rate, but changed with temperature (0.68 Pa·s at 135 °C and 0.11 Pa·s at 177.5 °C).  
295 The PMB had a behaviour similar to a Newtonian fluid as little to no difference was  
296 observed for the different temperatures applied, showing values from 3.21 Pa·s at 135 °C  
297 to 0.37 Pa·s at 177.5 °C. Of note, the PMB exceeded the value of 3 Pa·s at 135 °C  
298 prescribed by the Superpave™ specification. For a wide temperature range (from 135 up  
299 to 177.5 °C) CRMB, CRMB+GFA and CRMB+PCP showed similar viscosity values.  
300 Conversely, CRMB+AC exhibited a 45% higher viscosity on average for the same  
301 temperatures compared to the other CR modified blends. This is consistent with the stiffer

302 response observed in the penetration test. If a maximum viscosity of 3 Pa·s at 135 °C is  
 303 to be met, all blends modified with CR would pass this requirement, with the exception  
 304 of CRMB+AC. This would have to be heated to a temperature between 140 and 150 °C  
 305 to reach a viscosity of 3 Pa·s. As reported by Jamal et al. [56], the recommended  
 306 worldwide viscosity for CR specifications should be below a threshold that varies  
 307 between 1.5 and 4.0 Pa·s at 177.5 °C. In this case, all blends would easily pass this  
 308 requirement.



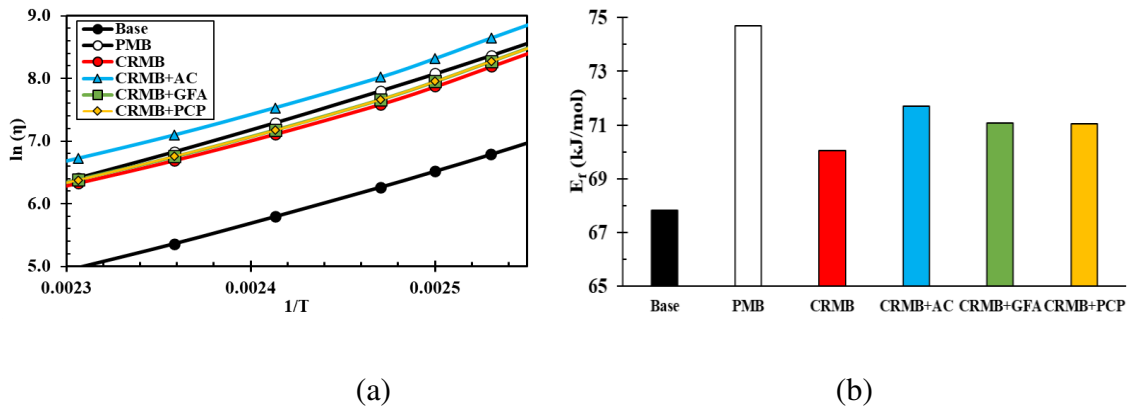
309

310 Note: Continuous red line: limit at 135 °C proposed by the Superpave™ specification. Dashed red line:  
 311 different limits for CRMB found in literature.

312 Figure 5. Viscosity measured with the cup and bob setup in the DSR for all samples at  
 313 different temperatures

314 Figure 6 plots  $\ln(\eta)$  versus  $1/T$  and the activation energy as determined by the slope of  
 315 their relationship. The results indicate that the incorporation of crumb rubber as a modifier  
 316 increased the activation energy, which results in an increased resistance to flow of the  
 317 binder. The addition of CR leads to the migration of bitumen oils into the CR particles  
 318 through diffusion causing swelling of CR particles, reducing inter-particle distance, thus  
 319 also increasing the viscosity of the bituminous component [57]. The addition of ERAs to  
 320 CRMB further increased the activation energy of the binder. Furthermore, it is worth

321 noting that among the three ERAs, AC increased the activation energy more than GFA  
 322 and PCP. This indicates that incorporating AC as an ERA leads to an increase in the  
 323 energy required to overcome the fluid resistance forces between the hydrocarbon chains,  
 324 which aligns with the findings from dynamic viscosity measurements.



325

326

327

328

Figure 6. (a) Ln of viscosity ( $\eta$ ) versus the inverse of temperature ( $1/T$ ) and (b) the activation energy ( $E_f$ ) for all binders

### 329 *Frequency sweeps*

330

331

332

333

334

335

336

337

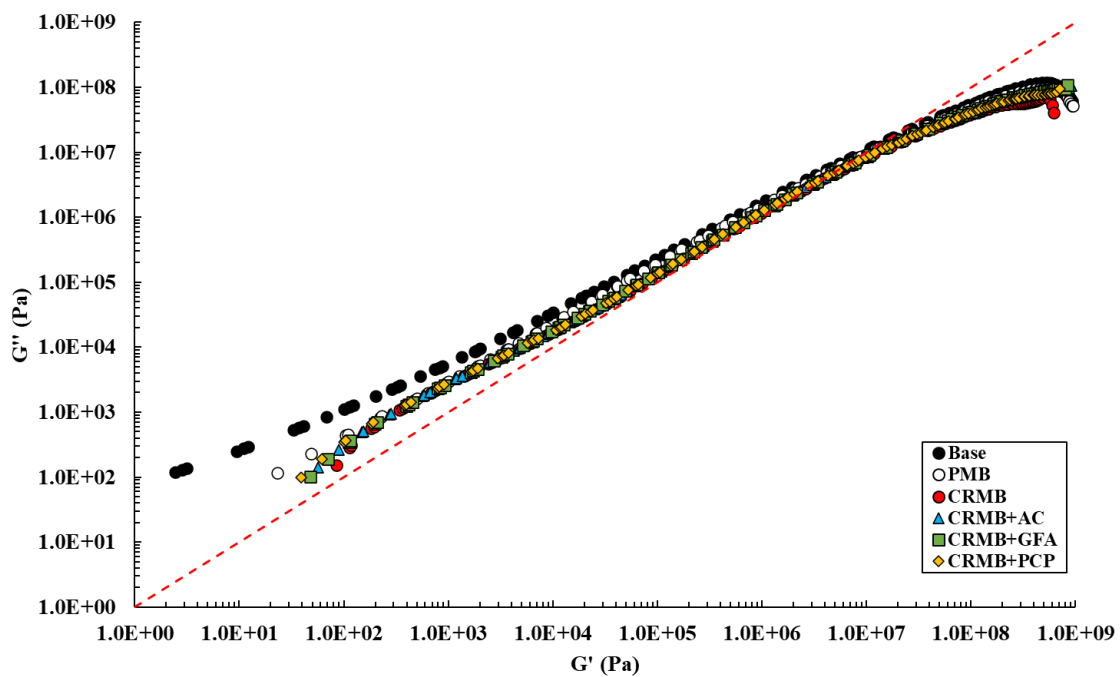
338

339

340

A Cole-Cole plot provides a graphical representation of the stiffness of a material and depicts the contribution of the material elastic (storage modulus –  $G'$ ) and viscous (loss modulus –  $G''$ ) components to its overall stiffness. The point at which  $G'$  equals the  $G''$  is known as the crossover frequency ( $\omega_c$ ), and its inverse is referred to as the relaxation time. Consequently, a line at a  $45^\circ$  angle indicates the position of the  $G' = G''$  points. Any points above this line exhibit a viscous-dominant phase, while points below the line display an elastic-dominant phase. The Cole-Cole plot for all blends is shown in Figure 7. In the case of the base binder, the lower stiffness range exhibited a significant proportion of the material response being governed by its viscous component. This indicates that the material behaves more like a liquid and loses its capacity to retain applied energy. Consequently, a substantial amount of this energy is dissipated, leading to a higher value

341 of  $G''$ . By incorporating CR into the base binder, both the overall stiffness and the ratio  
 342 of the elastic to the viscous components were increased, showing values similar to PMB,  
 343 particularly at lower stiffness values. The migration of bitumen oils into the CR particles  
 344 through diffusion, as previously mentioned, caused the binders modified with CR to  
 345 become stiffer. It can be seen that the addition of all ERAs had a minimal effect on the  
 346 relative contribution of the viscous and elastic components over the entire range of  
 347 stiffness values.

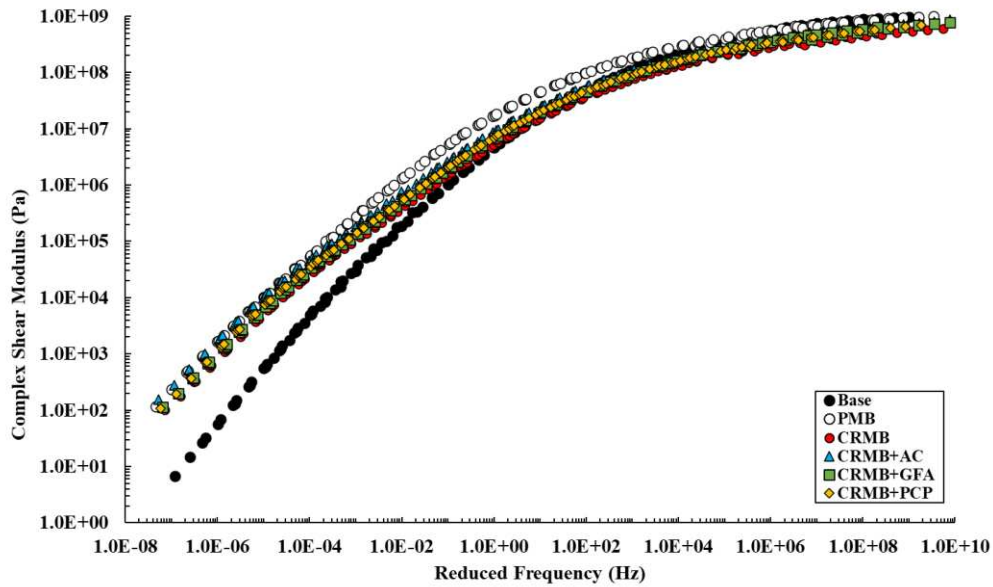


348

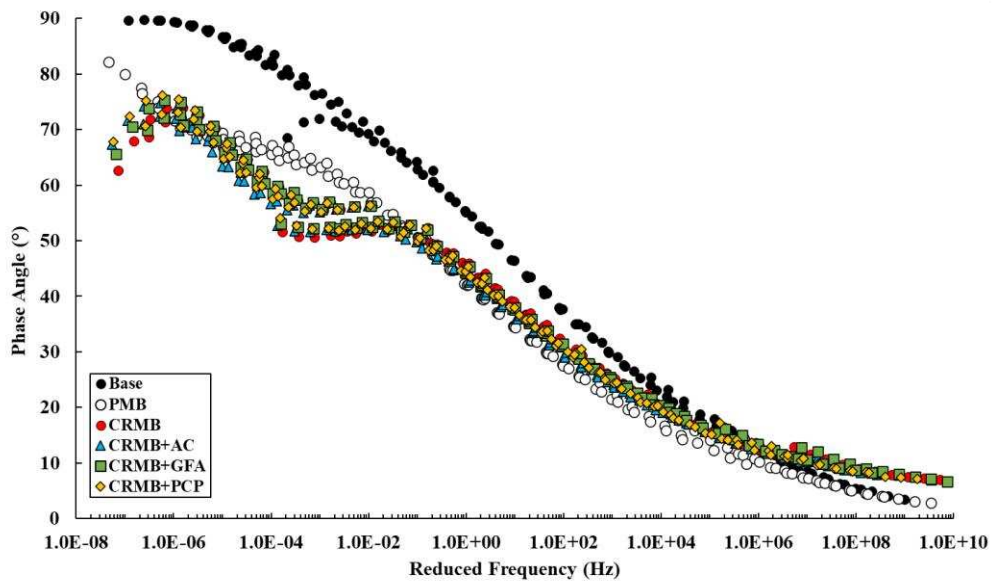
349 Figure 7. Cole-Cole plot for all blends

350 The complex shear modulus master curves of the samples are presented in Figure 8a. The  
 351 introduction of CR increased the stiffness of the binder in the lower frequency-high  
 352 temperature domain. This is advantageous from a performance standpoint as it improves  
 353 the resistance to rutting. Conversely, the complex shear modulus of CRMB was lower  
 354 than that of the base binder for the higher frequencies (low temperature domain). The  
 355 same behaviour was observed for the CRMB samples modified with ERAs, but with a  
 356 vertical shift in the  $G^*$  master curve, which can be translated as an increase in stiffness

357 for all temperatures/frequencies compared to CRMB. A flatter curve can also be seen for  
358 the CR modified blends, indicating a more gradual transition from a solid to a fluid state,  
359 as it represents the disparity between the glassy modulus and the modulus at the crossover  
360 frequency. Among all CR blends, CRMB+AC exhibited slightly higher complex shear  
361 moduli throughout the range of frequencies, which substantiates that the incorporation of  
362 AC contributed to increased stiffness and resistance to deformation.



(a)



(b)

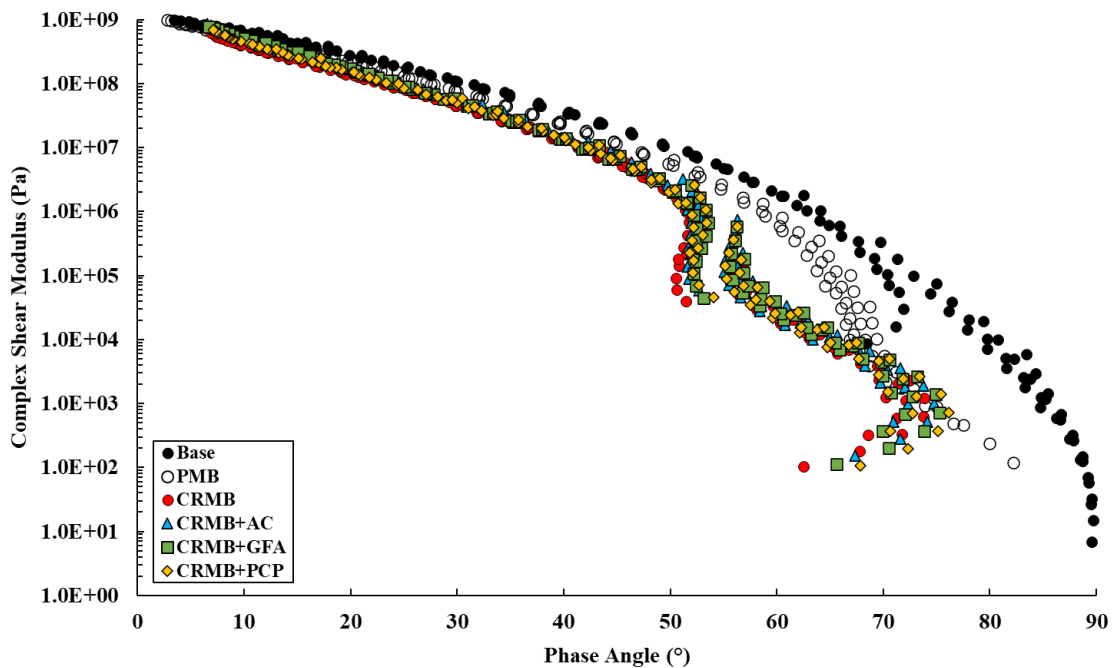
363 Figure 8. Influence of the use of ERAs and CR on the complex shear modulus (a) and  
364 phase angle (b) master curves

365 Figure 8b shows the phase angle master curves of all samples. The addition of CR reduced  
366 the phase angle throughout almost the entire range of frequencies, being rather  
367 remarkable at the lower frequencies (high-temperature domain). The lower phase angle  
368 at high temperatures indicates a more elastic response of the binder; hence the material  
369 can better recover its shape and resist deformation under dynamic loading conditions,  
370 which helps to reduce permanent deformation. A plateau is evident between the reduced  
371 frequencies of 1.0E-04 Hz and 1.0E-01 Hz for all CR modified binders. Notably, this  
372 plateau displays varying phase angle values at the same reduced frequencies. This  
373 demonstrates the dual-phase nature of the binder and the influence of the polymeric  
374 modification resulting from the presence of CR [41, 58]. The several phase angle values  
375 serve as a delineation between the bitumen-dominant phase and the polymer-dominant  
376 phase. To the right of this plateau, bitumen primarily governs the rheological behaviour  
377 and the blend characteristics resemble those of unmodified bitumen. However, at lower  
378 frequencies (high temperature domain), the base bitumen begins to soften, which makes  
379 the CR particles carry the shear load. The addition of the ERAs resulted in a slight lower  
380 phase angle at low to intermediate temperatures compared to CRMB. These results are in  
381 accordance with the findings reported by Cui et al. [25] and Wu et al. [26], who also  
382 found an increase in the complex shear modulus and a decrease in phase angle with the  
383 addition of CR and ERAs.

384 The CA-model yields additional parameters, namely  $\omega_c$  and R-value. Table 5 revealed a  
385 reduction in the crossover frequency and an increase in R-value of all the samples  
386 following the addition of CR. This decrease in  $\omega_c$  indicates that the binders modified with  
387 CR will require more time to relax stresses, specially for CRMB+AC, which may result

388 in the accumulation of residual stresses if the binder cannot rapidly dissipate applied  
 389 stresses. On the other hand, the elevation in R-value (similar values between CRMB and  
 390 samples with ERAs) signifies a flatter complex shear modulus master curve (as seen in  
 391 Figure 8a), which indicates a lower temperature dependency. Other studies have also  
 392 demonstrated that the R-value tends to rise with both polymer modification and binder  
 393 oxidation [59].

394 The Black diagrams shown in Figure 9 illustrate the rheological characteristics of the  
 395 CRMB blends, along with comparisons to the base and PMB binders. The curves for  
 396 PMB and the blends with CR exhibit distinct differences from that of the unmodified  
 397 bitumen. The curve of the base bitumen appears smoother than the trends displayed by  
 398 the modified bitumen, which agrees with the expectation that unmodified bitumen is  
 399 thermo-rheologically simpler [60].



400

401 Figure 9. Influence of the addition of CR and ERAs on the Black diagram.

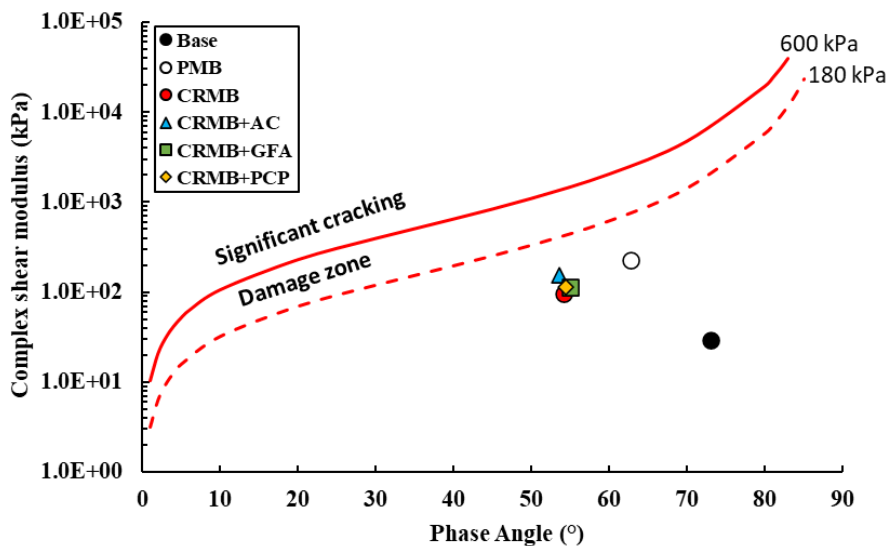
402 In the upper part of the Black diagram, where  $G^*$  is greater than 10 MPa, which represents  
 403 the low-temperature domain, the behaviour of the base bitumen and modified bitumen is



404 relatively similar. When comparing CRMB with the blends modified with ERAs, the  
405 addition of AC, PCP, and GFA did not significantly alter the rheological behaviour of  
406 CRMB besides the differences already mentioned for  $G^*$  and  $\delta$ . For  $G^*$  below 10 MPa  
407 (temperatures above 10 °C), the PMB and the CRMB blends yielded lower phase angles  
408 than the base binder, which substantiated a more elastic response. According to Airey  
409 [61], the influence of a polymer on bitumen is primarily significant at temperatures above  
410 10 °C. At these temperatures, the viscosity of the base bitumen decreases, which allows  
411 the elastic network of the polymer to primarily determine the mechanical properties of  
412 the blend. In addition, Airey et al. [62] demonstrated how the dominance of a polymer  
413 network of elastomeric SBS-modified bitumen exhibits a distinguishable elastic response  
414 at high testing temperatures. However, for CRMB and CRMB modified with ERAs, a  
415 rapid discontinuation after reaching a phase angle of approximately 50° was observed.  
416 This behaviour was also reported by Jamal et al. [57] and can be explained by the fact  
417 that when CR particles are added to bitumen, some are digested by the bituminous matrix  
418 while others remain insoluble. At low temperatures, the system consisting of undigested  
419 CR particles and bitumen with soluble CR particles acts as a single unit, resulting in lower  
420 overall stiffness than the base binder. As the temperature increases, the base binder  
421 undergoes a transition from a glassy state to a viscous solid and eventually to a viscous  
422 fluid. However, for CRMB, the bituminous phase softens and no longer acts as a single  
423 unit. The insoluble CR particles remain suspended without forming a long-range network  
424 due to the high viscosity of the surrounding phase around the CR particles, which restricts  
425 their motion. At this point, the bituminous phase contributes less to resisting external  
426 shearing forces, which are primarily sustained by the CR particles. This results in a  
427 sudden drop in the Black diagram.

428 The G-R parameter calculated for the unconditioned samples is presented in Table 5, and

429 the complex shear modulus and phase angle at 0.005 rad/s and 15 °C are plotted in Figure  
 430 10 alongside the G-R thresholds. All blends exhibit values well below the 180 kPa  
 431 threshold limit. The addition of CR increased in the G-R parameter close to the values for  
 432 PMB, which can be attributed to longer relaxation times, resulting in the accumulation of  
 433 residual stresses as the binder cannot rapidly dissipate applied stresses. When compared  
 434 to CRMB, the blends containing AC, GFA, and PCP showed an increase of 67%, 13%,  
 435 and 19% in G-R values, respectively. For all CRMB blends, the G-R parameter shifted  
 436 towards the upper left region of the graph, confirming that the addition of CR and ERA  
 437 increased the vulnerability to cracking, with the blend with AC being closer to the damage  
 438 zone.



439  
 440 Figure 10. Complex shear modulus and phase angle at 0.005 rad/s and 15°C plotted  
 441 with the G-R thresholds in a Black diagram

442  $\Delta T_c$  – Low temperature

443 Table 5 presents the results for  $T_{c,G}$ ,  $T_{c,m}$ , and  $\Delta T_c$ . The introduction of CR led to a  
 444 significant reduction in  $\Delta T_c$ , lowering it by nearly 6 °C and exceeding the critical limit of  
 445 -5 °C. Surprisingly, PMB also exhibited a lower  $\Delta T_c$  than the base binder, approaching  
 446 the critical limit. The incorporation of CR into the base binder slightly reduced  $T_{c,m}$ , with

447 the difference being minimal after the addition of ERAs. Conversely, the large shift in  
448  $T_{c,G}$  to colder temperatures explained the decrease in  $\Delta T_c$ . Thus, although  $T_{c,G}$  improved,  
449 the fact that  $T_{c,m}$  stayed relatively constant and  $\Delta T_c$  increased in absolute value makes it  
450 difficult to conclude if CR had a positive effect on low temperature performance. A  
451 similar trend was reported by Wititanapanit et al. [63] when comparing a control bitumen  
452 with samples modified with 3 and 7% natural rubber by weight of bitumen. The samples  
453 with ERA showed slightly warmer temperatures for  $T_{c,G}$  (3.2% to 9.6%) compared to  
454 CRMB, but still colder values than the base binder.

#### 455 *Linear amplitude sweep (LAS) – Intermediate temperature*

456 Table 5 summarises the strain values at failure ( $\gamma_f$ ), the peak stored strain energy (PSE),  
457 and the number of cycles to failure ( $N_{f,test}$ ) obtained from the LAS test. Notably, the  
458 addition of CR to the base binder increased the strain at failure by 32% and the maximum  
459 number of cycles to failure by 35%, indicating a superior fatigue performance. However,  
460 the addition of AC, GFA, and PCP reduced the performance of the CRMB as they showed  
461 lower values for  $\gamma_f$  and  $N_{f,test}$ . Of note, the CRMB+AC exhibited even inferior values than  
462 the base binder. Interestingly, PMB was the binder with the lowest  $\gamma_f$  and  $N_{f,test}$  but with  
463 the highest PSE. An explanation to the increase in performance provided by the CR could  
464 be that the additional strain experienced beyond the peak in shear stress activated the  
465 polymer network present in CR modified binders, enhancing the binder's capacity to  
466 accumulate energy during successive loading cycles and consequently increasing the  
467 number of cycles to failure.

#### 468 *Rutting Resistance Indicator (MSCR test) – High temperature*

469 The results at two stress levels (0.1 and 3.2 kPa) for the non-recoverable creep compliance

470 ( $J_{nr}$ ) and the percent recovery (%R) are presented in Table 5. The base binder used in this  
471 study has a softening point of just 51.8 °C, rendering it unsuitable for effectively resisting  
472 plastic permanent deformation at elevated temperatures and it can clearly be seen as a  
473 high non-recoverable deformation and low recovery. The addition of CR reduced  $J_{nr}$  to  
474 around 1/4th of its original value and increased %R significantly (55% and 57% for  $R_{0.1}$   
475 and  $R_{3.2}$ , respectively) to values more comparable to the ones for PMB, hence possibly  
476 improving rutting resistance. The addition of ERA did not show significant changes in  
477 the values for non-recoverable deformation and percent recovery when compared to the  
478 ones for CRMB.

## 479 **5. Finding and conclusions**

480 This study investigated the effect of emission reduction agents (ERAs) on the properties  
481 of crumb rubber modified bitumen (CRMB) and compared the results with the properties  
482 of a base binder and a polymer modified binder (PMB). Firstly, it was found that the  
483 addition of crumb rubber (CR) caused an overall stiffening effect on the base binder,  
484 which was substantiated by a lower penetration, a higher softening point and penetration  
485 index, increased viscosity, and a greater activation energy. In terms of rheology, the Cole-  
486 Cole plots, master curves, and MSCR results showed a more elastic response of the binder  
487 after adding CR, particularly in the high temperature-low frequency domain. Finally, CR  
488 seemed to reduce temperature dependency and improve the fatigue resistance at  
489 intermediate temperatures but it was unclear whether there was any benefit in terms of  
490 stress relaxation at lower temperatures.

491 Regarding the effect of ERAs on CRMB, it was concluded that all ERAs had an additional  
492 stiffening effect: penetration reduced and softening point, penetration index, and viscosity  
493 increased. This stiffening effect caused a significant drop in the fatigue resistance

494 measured in the LAS test. Out of the three ERAs evaluated, AC clearly induced the  
495 greatest changes in binder properties. However, MSCR results, crossover frequency, R-  
496 value, Glower-Rowe parameter, and  $\Delta T_c$  were less sensitive to the addition of ERAs.

497 When the results for CRMB+ERAs were compared with those for the base binder, it  
498 become evident that the incorporation of CR was the predominant factor influencing the  
499 characteristics of the modified blends, except for the LAS test, where the ERAs clearly  
500 had a strong effect on the fatigue response. When compared with the PMB, the  
501 CRMB+ERAs blends performed similarly in terms of both physical and rheological  
502 properties.

503 All in all, this study showed that the addition of ERAs like GFA and PCP did not impair  
504 the physical and rheological properties of CRMB, yielding results comparable to those of  
505 a PMB. However, the use of AC notably increased viscosity and worsened the fatigue  
506 response in the LAS test, which may introduce issues during mixing and service life.  
507 Future research should focus on assessing the environmental impact of CRMB with the  
508 incorporation of ERAs using life cycle assessment (LCA) to help make informed  
509 decisions about the best environmental option for CRMB production.

510 **Acknowledgments:** The authors thank the following companies for providing the materials for  
511 our research: bitumen from Total Energies Belgium N.V. and Total Bitumen Deutschland GmbH  
512 and crumb rubber from Rubber Recycling Overpelt (RRO). Furthermore, the authors  
513 acknowledge the support of iPRACS research groups (University of Antwerp, Belgium) for  
514 providing the Mastersize 2000 device.

## 515 **References**

- 516 [1] The Smithers Group Inc., The Future of Tire Manufacturing to 2024, 2020.  
517 [2] ETRMA, European Tyre & Rubber Industry Statistics Report, Belgium, 2021.

- 518 [3] Landi, D., Vitali, S., Germani, M., Environmental Analysis of Different End of Life  
519 Scenarios of Tires Textile Fibers, *Procedia CIRP* 48 (2016) 508-513.  
520 <https://doi.org/10.1016/j.procir.2016.03.141>
- 521 [4] ETRMA, End of Lyfe Tyre Report, European Tyre & Rubber Manufacturers'  
522 Association, Belgium, 2015.
- 523 [5] Zanetti, M.C., Fiore, S., Ruffino, B., Santagata, E., Dalmazzo, D., Lanotte, M.,  
524 Characterization of crumb rubber from end-of-life tyres for paving applications,  
525 *Waste Manage.* 45 (2015) 161-70. <https://doi.org/10.1016/j.wasman.2015.05.003>
- 526 [6] Xie, Z., Shen, J., Fatigue Performance of Rubberized Stone Matrix Asphalt by a  
527 Simplified Viscoelastic Continuum Damage Model, *J. Master Civ. Eng.* 28 (4)  
528 (2016). [https://doi.org/10.1061/\(ASCE\)MT.1943-5533.0001463](https://doi.org/10.1061/(ASCE)MT.1943-5533.0001463)
- 529 [7] Shirini, B., Imaninasab, R., Performance evaluation of rubberized and SBS modified  
530 porous asphalt mixtures, *Constr. Build. Mater.* 107 (2016) 165-171.  
531 <https://doi.org/10.1016/j.conbuildmat.2016.01.006>
- 532 [8] Yu, H., Leng, Z., Xiao, F., Gao, Z., Rheological and chemical characteristics of  
533 rubberized binders with non-foaming warm mix additives, *Constr. Build. Mater.*  
534 111 (2016) 671-678. <https://doi.org/10.1016/j.conbuildmat.2016.02.066>
- 535 [9] Lesueur, D., The colloidal structure of bitumen: Consequences on the rheology and  
536 on the mechanisms of bitumen modification, *Advances in colloid and interface*  
537 *science* 145(1-2) (2009) 42-82. <https://doi.org/10.1016/j.cis.2008.08.011>
- 538 [10] Mashaan, N.S., Ali, A.H., Karim, M.R., Abdelaziz, M., A review on using crumb  
539 rubber in reinforcement of asphalt pavement, *The Scientific World Journal* 2014  
540 (2014). <https://doi.org/10.1155/2014/214612>
- 541 [11] Borinelli, J.B., Blom, J., Portillo-Estrada, M., Kara De Maeijer, P., Van den Bergh,  
542 W., Vuye, C., VOC Emission Analysis of Bitumen Using Proton-Transfer  
543 Reaction Time-Of-Flight Mass Spectrometry, *Materials (Basel)* 13(17) (2020).  
544 <https://doi.org/10.3390/ma13173659>
- 545 [12] Pouranian, M.R., Shishehbor, M., Sustainability Assessment of Green Asphalt  
546 Mixtures: A Review, *Environments* 6(6) (2019).  
547 <http://doi.org/10.3390/environments6060073>
- 548 [13] Yang, X., You, Z., Perram, D., Hand, D., Ahmed, Z., Wei, W., Luo, S., Emission  
549 analysis of recycled tire rubber modified asphalt in hot and warm mix conditions,

- 550 J. Hazard. Mater. 365 (2019) 942-951.  
551 <https://doi.org/10.1016/j.jhazmat.2018.11.080>
- 552 [14] Wang, M., Wang, C., Huang, S., Yuan, H., Study on asphalt volatile organic  
553 compounds emission reduction: A state-of-the-art review, J. Clean. Prod. 318  
554 (2021). <https://doi.org/10.1016/j.jclepro.2021.128596>
- 555 [15] Borinelli, J.B., Portillo-Estrada, M., Oliveira Costa, J., Pajares, A., Blom, J.,  
556 Hernando, D., Vuye, C., Emission reduction agents: A solution to inhibit the  
557 emission of harmful volatile organic compounds from crumb rubber modified  
558 bitumen, Constr. Build. Mater. 411 (2024) 134455.  
559 <https://doi.org/10.1016/j.conbuildmat.2023.134455>
- 560 [16] Lin, S., Hung, W., Leng, Z., Air pollutant emissions and acoustic performance of hot  
561 mix asphalts, Constr. Build. Mater. 129 (2016) 1-10.  
562 <https://doi.org/10.1016/j.conbuildmat.2016.11.013>
- 563 [17] Chong, D., Wang, Y., Guo, H., Lu, Y., Volatile Organic Compounds Generated in  
564 Asphalt Pavement Construction and Their Health Effects on Workers, J. Constr.  
565 Eng. M. 140(2) (2014). [https://doi.org/10.1061/\(asce\)co.1943-7862.0000801](https://doi.org/10.1061/(asce)co.1943-7862.0000801)
- 566 [18] Celebi, U.B., Vardar, N., Investigation of VOC emissions from indoor and outdoor  
567 painting processes in shipyards, Atmospheric Environment 42(22) (2008) 5685-  
568 5695. <https://doi.org/10.1016/j.atmosenv.2008.03.003>
- 569 [19] Li, N., Jiang, Q., Wang, F., Cui, P., Xie, J., Li, J., Wu, S., Barbieri, D.M.,  
570 Comparative assessment of asphalt volatile organic compounds emission from  
571 field to laboratory, J. Clean. Prod. 278 (2021) 123479.  
572 <https://doi.org/10.1016/j.jclepro.2020.123479>
- 573 [20] Bostancıoğlu, M., Oruç, Ş., Effect of activated carbon and furan resin on asphalt  
574 mixture performance, Road Mater. Pavement. 17(2) (2016) 512-525.  
575 <https://doi.org/10.1080/14680629.2015.1092465>
- 576 [21] Guo, F., Zhang, J., Pei, J., Zhou, B., Falchetto, A.C., Hu, Z., Investigating the  
577 interaction behavior between asphalt binder and rubber in rubber asphalt by  
578 molecular dynamics simulation, Constr. Build. Mater. 252 (2020).  
579 <https://doi.org/10.1016/j.conbuildmat.2020.118956>
- 580 [22] Turbay, E., Martinez-Arguelles, G., Navarro-Donado, T., Sanchez-Cotte, E., Polo-  
581 Mendoza, R., Covilla-Valera, E., Rheological Behaviour of WMA-Modified

- 582 Asphalt Binders with Crumb Rubber, *Polymers* (Basel) 14(19) (2022).  
583 <https://doi.org/10.3390/polym14194148>
- 584 [23] Yu, X., Leng, Z., Wang, Y., Lin, S., Characterization of the effect of foaming water  
585 content on the performance of foamed crumb rubber modified asphalt, *Constr.*  
586 *Build. Mater.* 67 (2014) 279-284.  
587 <https://doi.org/10.1016/j.conbuildmat.2014.03.046>
- 588 [24] Xiu, M., Wang, X., Morawska, L., Pass, D., Beecroft, A., Mueller, J.F., Thai, P.,  
589 Emissions of particulate matters, volatile organic compounds and polycyclic  
590 aromatic hydrocarbons from warm and hot asphalt mixes, *J. Clean. Prod.* 275  
591 (2020). <https://doi.org/10.1016/j.jclepro.2020.123094>
- 592 [25] Cui, P., Wu, S., Li, F., Xiao, Y., Zhang, H., Investigation on Using SBS and Active  
593 Carbon Filler to Reduce the VOC Emission from Bituminous Materials, *Materials*  
594 (Basel) 7(9) (2014) 6130-6143. <https://doi.org/10.3390/ma7096130>
- 595 [26] Wu, S., Ye, Y., Shu, B., Li, Y., Li, C., Kong, D., Liu, Q., Xie, J., Synthesis and  
596 utilization of mesoporous hollow silica particles for bitumen, *Journal of Testing*  
597 *and Evaluation* 48(3) (2019) 2093-2103. <https://doi.org/10.1520/JTE20190208>
- 598 [27] PubChem National Center for Biotechnology Information, U. S. National Library of  
599 Medicine, Bethesda, MD, USA, 2022.
- 600 [28] Bressi, S., Fiorentini, N., Huang, J., Losa, M., Crumb Rubber Modifier in Road  
601 Asphalt Pavements: State of the Art and Statistics, *Coatings* 9(6) (2019) 384.  
602 <https://doi.org/10.3390/coatings9060384>
- 603 [29] Lo Presti, D., Recycled Tyre Rubber Modified Bitumens for road asphalt mixtures:  
604 A literature review, *Constr. Build. Mater.* 49 (2013) 863-881.  
605 <https://doi.org/10.1016/j.conbuildmat.2013.09.007>
- 606 [30] Duan, H., Zhu, C., Li, Y., Zhang, H., Zhang, S., Xiao, F., Amirkhanian, S., Effect of  
607 crumb rubber percentages and bitumen sources on high-temperature rheological  
608 properties of less smell crumb rubber modified bitumen, *Constr. Build. Mater.*  
609 277 (2021) 122248. <https://doi.org/10.1016/j.conbuildmat.2021.122248>
- 610 [31] Borinelli, J.B., Blom, J., Jacobs, G., Hernando, D., Van den Bergh, W., Vuye, C.,  
611 Microstructural and rheological analysis of crumb rubber modified bitumen,  
612 *Green and Intelligent Technologies for Sustainable and Smart Asphalt Pavements*  
613 (2021) 599-604. <https://doi.org/10.1201/9781003251125-96>



- 614 [32] Long, Y., Wu, S., Xiao, Y., Cui, P., Zhou, H., VOCs reduction and inhibition  
615 mechanisms of using active carbon filler in bituminous materials, *J. Clean. Prod.*  
616 181 (2018) 784-793. <https://doi.org/10.1016/j.jclepro.2018.01.222>
- 617 [33] Tang, N., Deng, Z., Dai, J.-G., Yang, K., Chen, C., Wang, Q., Geopolymer as an  
618 additive of warm mix asphalt: Preparation and properties, *J. Clean. Prod.* 192  
619 (2018) 906-915. <https://doi.org/10.1016/j.jclepro.2018.04.276>
- 620 [34] Pfeiffer, J.P., Van Doormaal, P., The rheological properties of asphaltic bitumens,  
621 *Journal of the Institute of Petroleum Technologists* 22 (1936) 414-440.
- 622 [35] Wang, H., Liu, X., Apostolidis, P., Scarpas, T., Non-Newtonian Behaviors of Crumb  
623 Rubber-Modified Bituminous Binders, *Applied Sciences* 8(10) (2018).  
624 <https://doi.org/10.3390/app8101760>
- 625 [36] Pouranian, M.R., Notani, M.A., Tabesh, M.T., Nazeri, B., Shishehbor, M.,  
626 Rheological and environmental characteristics of crumb rubber asphalt binders  
627 containing non-foaming warm mix asphalt additives, *Constr. Build. Mater.* 238  
628 (2020). <https://doi.org/10.1016/j.conbuildmat.2019.117707>
- 629 [37] Abatech, Rheology Analysis Software, Blooming Glen, PA, 2011.
- 630 [38] Anderson, D.A., Christensen, D.W., Bahia, H.U., Dongre, R., Sharma, M., Antle,  
631 C.E., Button, J., Binder characterization and evaluation, volume 3: Physical  
632 characterization, Strategic Highway Research Program, National Research  
633 Council, Washington, DC, 1994.
- 634 [39] Christensen, D.W., Anderson, D.A., Interpretation of dynamic mechanical test data  
635 for paving grade asphalt cements (with discussion), *Journal of the Association of*  
636 *Asphalt Paving Technologists* 61 (1992).
- 637 [40] Rowe, G.M., Barry, J., Crawford, K., Evaluation of a 100% rap recycling project in  
638 Fort Wayne, Indiana, 8th RILEM international symposium on testing and  
639 characterization of sustainable and innovative bituminous materials, Springer,  
640 2016, pp. 941-951.
- 641 [41] Airey, G.D., Use of black diagrams to identify inconsistencies in rheological data,  
642 *Road Mater. Pavement.* 3(4) (2002) 403-424.  
643 <https://doi.org/10.1080/14680629.2002.9689933>
- 644 [42] Glover, C.J., Davison, R.R., Domke, C.H., Ruan, Y., Juristyarini, P., Knorr, D.B.,  
645 Jung, S.H., Development of a new method for assessing asphalt binder durability  
646 with field validation, Texas Dept Transport, 2005, pp. 1-334.

- 647 [43] Rowe, G., King, G., Anderson, M., The influence of binder rheology on the cracking  
648 of asphalt mixes in airport and highway projects, *Journal of Testing and*  
649 *Evaluation* 42(5) (2014) 1063-1072. <https://doi.org/10.1520/JTE20130245>
- 650 [44] Rowe, G., Prepared discussion for the AAPT paper by Anderson et al.: Evaluation  
651 of the relationship between asphalt binder properties and non-load related  
652 cracking, *Journal of the Association of Asphalt Paving Technologists* 80 (2011)  
653 649-662.
- 654 [45] Elkashef, M., Podolsky, J., Williams, R.C., Cochran, E., Preliminary examination of  
655 soybean oil derived material as a potential rejuvenator through Superpave criteria  
656 and asphalt bitumen rheology, *Constr. Build. Mater.* 149 (2017) 826-836.  
657 <https://doi.org/10.1016/j.conbuildmat.2017.05.195>
- 658 [46] Hao, G., Huang, W., Yuan, J., Tang, N., Xiao, F., Effect of aging on chemical and  
659 rheological properties of SBS modified asphalt with different compositions,  
660 *Constr. Build. Mater.* 156 (2017) 902-910.  
661 <https://doi.org/10.1016/j.conbuildmat.2017.06.146>
- 662 [47] Anderson, R.M., King, G.N., Hanson, D.I., Blankenship, P.B., Evaluation of the  
663 relationship between asphalt binder properties and non-load related cracking,  
664 *Journal of the Association of Asphalt Paving Technologists* 80 (2011).
- 665 [48] Christensen, D., Mensching, D., Rowe, G., Anderson, R.M., Hanz, A., Reinke, G.,  
666 Anderson, D., Past, present, and future of asphalt binder rheological parameters:  
667 Synopsis of 2017 Technical Session 307 at the 96th Annual Meeting of the  
668 Transportation Research Board, *Transportation Research Circular (E-C241)*  
669 (2019).
- 670 [49] Sui, C., Farrar, M.J., Harnsberger, P.M., Tuminello, W.H., Turner, T.F., New low-  
671 temperature performance-grading method: Using 4-mm parallel plates on a  
672 dynamic shear rheometer, *Transport. Res. Rec.* 2207(1) (2011) 43-48.  
673 <https://doi.org/10.3141/2207-06>
- 674 [50] Bahia, H.U., Zhai, H., Zeng, M., Hu, Y., Turner, P., Development of binder  
675 specification parameters based on characterization of damage behavior (with  
676 discussion), *Journal of the Association of Asphalt Paving Technologists* 70  
677 (2001).
- 678 [51] Cao, W., Mohammad, L.N., Barghabany, P., Use of viscoelastic continuum damage  
679 theory to correlate fatigue resistance of asphalt binders and mixtures, *Int. J.*

- 680 Geomech 18(11) (2018) 04018151. [https://doi.org/10.1061/\(ASCE\)GM.1943-](https://doi.org/10.1061/(ASCE)GM.1943-)  
681 [5622.0001306](https://doi.org/10.1061/(ASCE)GM.1943-5622.0001306)
- 682 [52] Safaei, F., Castorena, C., Kim, Y.R., Linking asphalt binder fatigue to asphalt  
683 mixture fatigue performance using viscoelastic continuum damage modeling,  
684 Mechanics of Time-Dependent Materials 20(3) (2016) 299-323.  
685 <https://doi.org/10.1007/s11043-016-9304-1>
- 686 [53] Safaei, F., Castorena, C., Material nonlinearity in asphalt binder fatigue testing and  
687 analysis, Materials & Design 133 (2017) 376-389.  
688 <https://doi.org/10.1016/j.matdes.2017.08.010>
- 689 [54] Yan, Y., Hernando, D., Park, B., Allen, C., Roque, R., Understanding asphalt binder  
690 cracking characterization at intermediate temperatures: Review and evaluation of  
691 two approaches, Constr. Build. Mater. 312 (2021).  
692 <https://doi.org/10.1016/j.conbuildmat.2021.125163>
- 693 [55] Tang, N., Yang, K.-k., Alrefaei, Y., Dai, J.-G., Wu, L.-M., Wang, Q., Reduce VOCs  
694 and PM emissions of warm-mix asphalt using geopolymers additives, Constr.  
695 Build. Mater. 244 (2020). <https://doi.org/10.1016/j.conbuildmat.2020.118338>
- 696 [56] Jamal, M., Giustozzi, F., Chemo-rheological Investigation on Waste Rubber-  
697 Modified Bitumen Response to Various Blending Factors, International Journal  
698 of Pavement Research and Technology 15(2) (2021) 395-414.  
699 <https://doi.org/10.1007/s42947-021-00045-x>
- 700 [57] Jamal, M., Giustozzi, F., Low-content crumb rubber modified bitumen for improving  
701 Australian local roads condition, J. Clean. Prod. 271 (2020).  
702 <https://doi.org/10.1016/j.jclepro.2020.122484>
- 703 [58] Soenen, H., Lu, X., Redelius, P., The Morphology of Bitumen-SBS Blends by UV  
704 Microscopy: an evaluation of preparation methods, Road Mater. Pavement. 9(1)  
705 (2008) 97-110. <https://doi.org/10.1080/14680629.2008.9690109>
- 706 [59] Booshehrian, A., Mogawer, W.S., Bonaquist, R., How to construct an asphalt binder  
707 master curve and assess the degree of blending between RAP and virgin binders,  
708 J. Mater. Civil. Eng. 25(12) (2013) 1813-1821.  
709 [https://doi.org/10.1061/\(ASCE\)MT.1943-5533.000072](https://doi.org/10.1061/(ASCE)MT.1943-5533.000072)
- 710 [60] Kaya, D., Topal, A., McNally, T., Relationship between processing parameters and  
711 aging with the rheological behaviour of SBS modified bitumen, Constr. Build.  
712 Mater. 221 (2019) 345-350. <https://doi.org/10.1016/j.conbuildmat.2019.06.081>

- 713 [61] Airey, G.D., Rheological evaluation of ethylene vinyl acetate polymer modified  
714 bitumens, *Constr. Build. Mater.* 16(8) (2002) 473-487.  
715 [https://doi.org/10.1016/S0950-0618\(02\)00103-4](https://doi.org/10.1016/S0950-0618(02)00103-4)
- 716 [62] Airey, G.D., Singleton, T.M., Collop, A.C., Properties of Polymer Modified Bitumen  
717 after Rubber-Bitumen Interaction, *J. Mater. Civil. Eng.* 14(4) (2002) 344-354.  
718 [https://doi.org/10.1061/\(asce\)0899-1561\(2002\)14:4\(344\)](https://doi.org/10.1061/(asce)0899-1561(2002)14:4(344))
- 719 [63] Wititanapanit, J., Carvajal-Munoz, J.S., Airey, G., Performance-related and  
720 rheological characterisation of natural rubber modified bitumen, *Constr. Build.*  
721 *Mater.* 268 (2021) 121058. <https://doi.org/10.1016/j.conbuildmat.2020.121058>  
722